JACS
JOURNAL OF THE AMERICAN CHEMICAL SOCIETY
Communication
pubs.acs.org/JACS

# Cation-Dependent Intrinsic Electrical Conductivity in Isostructural Tetrathiafulvalene-Based Microporous Metal–Organic Frameworks

Sarah S. Park,[†] Eric R. Hontz,[†] Lei Sun,[†] Christopher H. Hendon,[‡] Aron Walsh,[‡] Troy Van Voorhis,[†] and Mircea Dincă*[,†]

[†]Department of Chemistry, Massachusetts Institute of Technology, 77 Massachusetts Avenue, Cambridge, Massachusetts 02139, United States

[‡]Department of Chemistry, University of Bath, Claverton Down, Bath BA2 7AY, United Kingdom

Supporting Information

**ABSTRACT:** Isostructural metal–organic frameworks (MOFs) $M_2$(TTFTB) (M = Mn, Co, Zn, and Cd; $H_4$TTFTB = tetrathiafulvalene tetrabenzoate) exhibit a striking correlation between their single-crystal conductivities and the shortest S···S interaction defined by neighboring TTF cores, which inversely correlates with the ionic radius of the metal ions. The larger cations cause a pinching of the S···S contact, which is responsible for better orbital overlap between $p_z$ orbitals on neighboring S and C atoms. Density functional theory calculations show that these orbitals are critically involved in the valence band of these materials, such that modulation of the S···S distance has an important effect on band dispersion and, implicitly, on the conductivity. The Cd analogue, with the largest cation and shortest S···S contact, shows the largest electrical conductivity, $\sigma$ = 2.86 (±0.53) × $10^{-4}$ S/cm, which is also among the highest in microporous MOFs. These results describe the first demonstration of tunable intrinsic electrical conductivity in this class of materials and serve as a blueprint for controlling charge transport in MOFs with $\pi$-stacked motifs.

Imbuing metal–organic frameworks (MOFs) with properties that complement their porosity will add a new dimension to the range of potential applications for these materials.[1] Chief among these would be those that employ the extended nature of the MOFs' structures to impart emerging properties that are not available in the molecular precursors. Cooperative magnetism, exciton transport, or charge transport phenomena are some examples that are slowly emerging along this line.[2] Among these, electrical conductivity is particularly difficult to engineer in MOFs[3] because these materials generally have flat bands determined by highly localized organic states and weak hybridization with the inorganic secondary building units (SBUs). Indeed, of the many hundreds of microporous MOFs, only a few exhibit intrinsic conductivity.[4] Nevertheless, should electrical conductivity be enabled in such materials, their crystalline structures may provide highly ordered and nearly defect-free infinite charge transport pathways,[5] leading to superior electrical properties relative to typical conductive polymers, which suffer from chain recoiling and disorder that limit their charge mobility.[6] The challenge, then, sits squarely in the realm of synthetic chemistry: how can one control the supramolecular arrangement of molecular building blocks to enable electrical conductivity in a microporous MOF?

Three charge transport mechanisms can be operative in molecular conductors such as MOFs: one relies on $\pi$-stacking (through-space charge transport); another involves charge transport through the covalent bonds, as in molecular wires; and the third is charge hopping.[7−10] The first two mechanisms are ideally based on band transport, while the hopping mechanism is governed by Marcus theory.[11] Recently, it has been shown that all three mechanisms can be exploited to synthesize MOFs with excellent intrinsic charge mobility and conductivity. Tetrathiafulvalene tetrabenzoic acid ($H_4$TTFTB) forms a zinc MOF with infinite $\pi$-stacked TTF columns that shows a charge mobility of 0.2 $cm^2/V{\cdot}s$, as determined by time-resolved microwave conductivity.[12] Triazole- and sulfur-ligated MOFs, such as metal triazolates,[13] $Mn_2$(DSBDC) (DSBDC = 2,5-disulfhydrylterephthalate)[4f] and Cu[Ni(pdt)$_2$] ($pdt^{2-}$ = pyrazine-2,3-dithiolate),[14] have also shown promising electrical properties. Recent work has also highlighted the excellent properties of two-dimensional graphite-like materials,[15] with $Ni_3$(HITP)$_2$ (HITP = hexaiminotriphenylene) reaching the same bulk conductivity as graphite.[16]

One of the more exciting aspects of producing conductive MOFs, in addition to their potential utility in electronic devices, is the ability to tune their electrical properties. This has been shown with $Cu_3$(BTC)$_2$ (BTC = 1,3,5-benzenetricarboxylate), for instance, whose conductivity can be tuned by six orders of magnitude when various amounts of tetracyanoquinodimethane (TCNQ) are introduced in the pores.[5b] To our knowledge, there are no examples where the conductivity of a MOF can be tuned in the absence of intentional doping or other external factors that often reduce the available surface area by pore blocking. Here, we show that varying the metal cation employed in the synthesis of TTFTB-based MOFs from $Zn^{2+}$ to $Co^{2+}$, $Mn^{2+}$, and $Cd^{2+}$ changes the shortest S···S distance between neighboring TTF cores in the infinite $\pi$-stacked columns. This causes a modulation of the single-crystal conductivity by nearly 2 orders of magnitude in the absence of any other external variables. The variation correlates very well with the S···S distance and is confirmed by conductivity measurements of over 20 single crystals for each sample.

**Received:** December 5, 2014
**Published:** January 18, 2015





DOI: 10.1021/ja512437u
J. Am. Chem. Soc. 2015, 137, 1774−1777

As previously reported, reaction of $H_4$TTFTB with $Zn(NO_3)_2$ produces $Zn_2$(TTFTB), wherein TTF ligands form a chiral $\pi$-stack with $6_5$ symmetry and are connected to infinite zinc benzoate chains (Figure 1b). Because $\pi-\pi$ interactions are weaker than covalent interactions, we surmised that changing the metal cation would maintain the overall structure of the covalent lattice. At the same time, we hypothesized that increasing the ionic radius of the metal cation would lengthen the metal–carboxylate chains, thereby possibly pinching the TTF stack, leading to a shorter intermolecular S···S distance. Decreasing this parameter would increase the dispersion of the band formed by the sulfur $3p_z$ orbitals because it would increase the overlap integral for these orbitals.[17] Overall, this should have a positive effect on the electrical properties of isostructural MOFs made with cations of increasing radius.

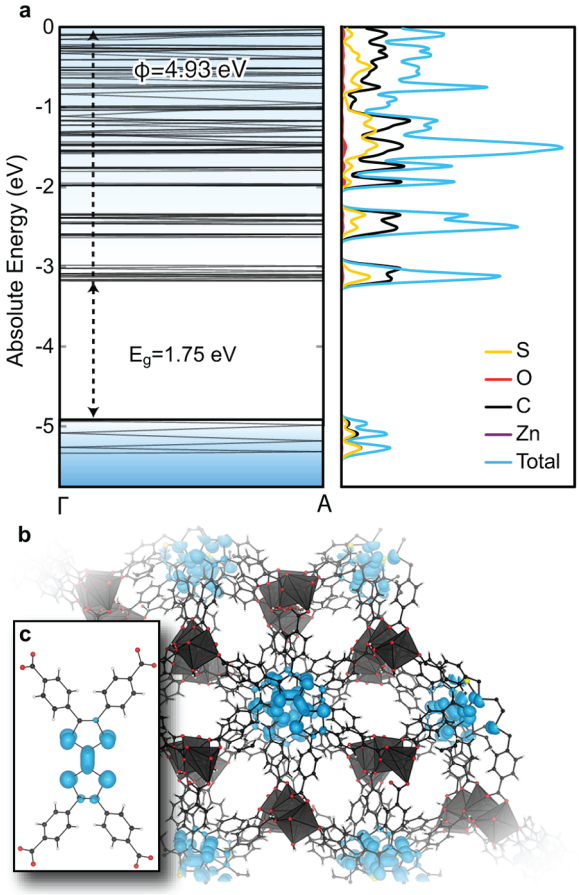


**Figure 1.** (a) Calculated band structure and projected density of states of $Zn_2$(TTFTB). The work function, $\phi$, and absolute energy scale are aligned to vacuum according to ref 20. The coordinates of the reciprocal space points are Γ = (0, 0, 0) and A = (0, 0, 1/2). Corresponding pictorial representation of the valence band orbitals in $Zn_2$(TTFTB) (b) and one of the TTF cores (c). Zn atoms and their coordination sphere are represented by black polyhedra. Gold, red, black, and white spheres represent S, O, C, and H atoms, respectively.

To verify these hypotheses, we employed density functional theory to calculate the band structure of the reported $Zn_2$(TTFTB) material. Several important facts emerge from this calculation, which is shown in Figure 1. First, the width of the upper valence band is 400 meV. This is much larger than that reported for many other MOFs,[18] whose bands are so narrow that they may be more prosaically described as discrete energy levels.[19] The valence band is also considerably wider than the conduction band, as expected for a hole conductor based on electron-donating TTF units. Finally, the p orbitals of the sulfur and central carbon atoms on TTF define the valence band, suggesting that indeed the likely pathway for charge transport involves these orbitals and that, according to the extended Hückel theory, the band dispersion of a TTF stack would be dramatically varied as the overlap of these p orbitals changes. A qualitatively similar picture is observed for the Cd analogue of this material (vide infra and Figure S1).

Reacting $H_4$TTFTB with $Mn(NO_3)_2{\cdot}xH_2O$, $Co(NO_3)_2{\cdot}6H_2O$, or $Cd(NO_3)_2{\cdot}4H_2O$ under conditions mimicking those used for the synthesis of $Zn_2$(TTFTB) produced $[Mn_2(C_{34}H_{16}O_8S_4)(H_2O)_2]{\cdot}(DMF)_{0.7}(H_2O)_{1.75}$ (Mn$_2$(TTFTB)), $[Co_2(C_{34}H_{16}O_8S_4)(H_2O)_2]{\cdot}(DMF)_{1.75}(H_2O)_2$ ($Co_2$(TTFTB)), and $[Cd_2(C_{34}H_{16}O_8S_4)(\mu_2\text{-}OH_2)(H_2O)]{\cdot}(DMF)_{1.5}(H_2O)_2$ ($Cd_2$(TTFTB)) as dark red needles. Powder X-ray diffraction confirmed the homogeneity of the bulk crystalline samples, which are all isostructural with $Zn_2$(TTFTB) (Figure S2). Single-crystal X-ray diffraction confirmed that all three compounds crystallize in the $P6_5$ space group, where the $6_5$ screw axis is slightly offset from the central ethylene unit of the TTF core, such that the TTF units are rotated by 60° relative to one another and translated in the $c$ direction (Figure 2). The plane containing the TTF core is not perfectly perpendicular to the screw axis, which results in only one relatively close S···S contact between each pair of neighboring TTF units. SBUs are helical chains of corner-sharing metal–oxygen polyhedra joined by helical stacks of benzoates pertaining to $TTFTB^{4-}$. Whereas the Zn, Co, and Mn materials exhibit corner-sharing pseudo-octahedra, $Cd_2$(TTFTB) exhibits alternating seven- and six-coordinate metal ions.

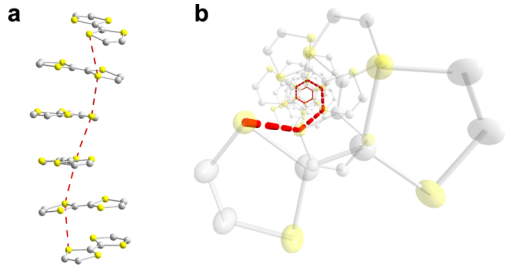


**Figure 2.** Helical TTF stack with a depiction of the shortest intermolecular S···S contacts (dashed red line): (a) view along the $ab$ plane; (b) view down the $c$ axis. Yellow and gray spheres represent S and C atoms, respectively. Phenyl rings and metal atoms were omitted for clarity.

Thermogravimetric analysis coupled with elemental analysis of samples desolvated at 200 °C and 4 mTorr showed that Mn$_2$(TTFTB) and $Co_2$(TTFTB) lose both coordinated and guest solvent molecules, while $Cd_2$(TTFTB) loses the coordinated water molecules only above ~220 °C (Figure S3). All show permanent microporosity evidenced by $N_2$ adsorption isotherms at 77 K, which revealed uptakes of ~150, ~170, and ~140 $cm^3/g$ of $N_2$ and BET surface areas of 470, 531, and 521 $m^2/mmol$, respectively for Mn$_2$(TTFTB), $Co_2$(TTFTB), and $Cd_2$(TTFTB) (Figure S4). These are comparable with the surface area of $Zn_2$(TTFTB) (537 $m^2/mmol$).

Most importantly, the shortest S···S distance observed in each of the materials follows the predicted pattern and increases from


DOI: 10.1021/ja512437u
J. Am. Chem. Soc. 2015, 137, 1774–1777

3.6538(23) Å in $Cd_2$(TTFTB) to 3.6929(6), 3.7568(13), and 3.7732(26) Å in $Mn_2$(TTFTB), $Zn_2$(TTFTB), and $Co_2$(TTFTB), respectively. The respective ionic radii vary inversely from 109 pm for $Cd^{2+}$ to 97, 88, and 88.5 pm for high-spin $Mn^{2+}$, $Zn^{2+}$, and $Co^{2+}$.[21] These values are summarized in Table 1. These short intermolecular S···S distances are

**Table 1. Closest Interatomic S···S Distance between Neighboring TTF Cores**

| | ionic radius of $M^{II}$ (pm) | S···S (Å) |
|---|---|---|
| $Co_2$(TTFTB) | 88.5 | 3.7732(26) |
| $Zn_2$(TTFTB) | 88 | 3.7568(13) |
| $Mn_2$(TTFTB) | 97 | 3.6929(6) |
| $Cd_2$(TTFTB) | 109 | 3.6538(23) |

comparable to those found in charge transfer salts such as TTF-TCNQ ($d_{S\cdots S}$ = 3.75 Å),[22] TTF-dicyanoquinodiimine ($d_{S\cdots S}$ = 3.69 Å),[23] and $TTF_3Cl$ ($d_{S\cdots S}$ = 3.60 Å).[24]

To assess the influence of the S···S separation on the intrinsic electrical properties of each material, we performed single-crystal conductivity measurements, which are less affected by grain boundaries than bulk pellet measurements (see Supporting Information for experimental details). Because conductivity is the product of charge mobility and charge carrier density and the width of the valence band was expected to influence the mobility but not the carrier density, we needed to estimate the latter in each case. To this end, it is well-known that the lengths of the C−S and C═C bonds in TTF are sensitive to the level of doping in stacked TTF materials.[25] As shown in Table S4, we found that among the $M_2$(TTFTB) materials these bonds vary by less than 0.0025 and 0.019 Å for the C−S and C═C bonds, respectively. Although small variations in charge carrier densities associated with slightly different positions of the Fermi level may not be apparent in these distances and may yet influence conductivity, this analysis suggests that the level of doping is similar in each material.

Single crystal conductivity measurements were performed along the crystallographic *c* axis of millimeter-sized needle-shaped crystals, using two gold probes attached by carbon paste at each end of a crystal.[26] Current−voltage curves were measured by sweeping the voltage from −1 to 1 V. Ohmic contacts were observed in this potential interval. To eliminate variations stemming from batch/device preparation and microscopic defects, we performed measurements on more than 20 crystals coming from 4−5 independent batches for each $M_2$(TTFTB) variant. A histogram of the results is shown in Figure 3. Average conductivity values obtained under these conditions, plotted against the observed S···S distance in Figure 4, show a remarkable variation among the four isostructural MOFs. $Cd_2$(TTFTB), which exhibits the shortest S···S distance, has an average conductivity of 2.86 (±0.53) × $10^{-4}$ S/cm. This is 72 times higher than the average conductivity of $Zn_2$(TTFTB) ($\sigma$ = 3.95 (±0.56) × $10^{-6}$ S/cm). $Mn_2$(TTFTB) and $Co_2$(TTFTB), which display intermediate S···S distances between those observed in the Zn and Cd analogues, also show intermediate conductivity values of 8.64 (±1.21) × $10^{-5}$ and 1.49 (±0.29) × $10^{-5}$ S/cm, respectively, both tracking inversely with increasing S···S distance. We note that four-point probe conductivity measurements of single crystals of $Cd_2$(TTFTB), $Mn_2$(TTFTB), and $Co_2$(TTFTB) revealed values of 6.79 × $10^{-4}$, 1 × $10^{-4}$, and 5 × $10^{-5}$ S/cm, respectively. These show a trend that is in line with that observed by two-probe measurements, suggesting that

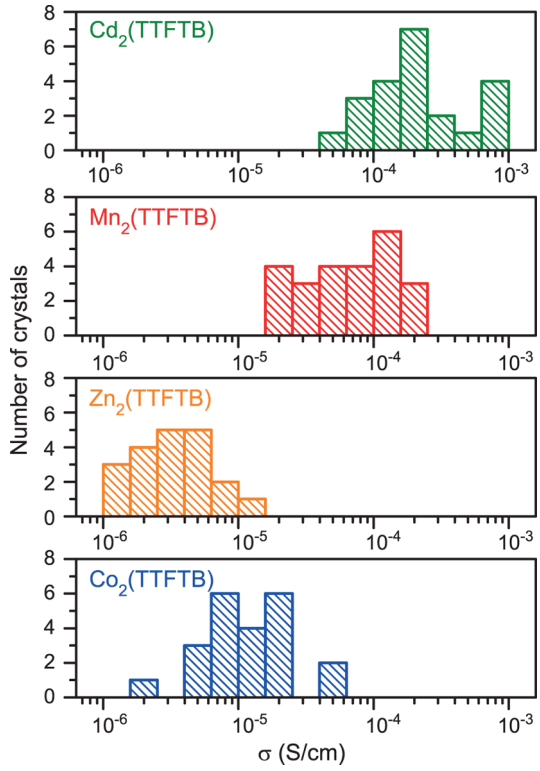


**Figure 3.** Histograms with the distribution of single crystal electrical conductivities for $Cd_2$(TTFTB), $Mn_2$(TTFTB), $Zn_2$(TTFTB), and $Co_2$(TTFTB).

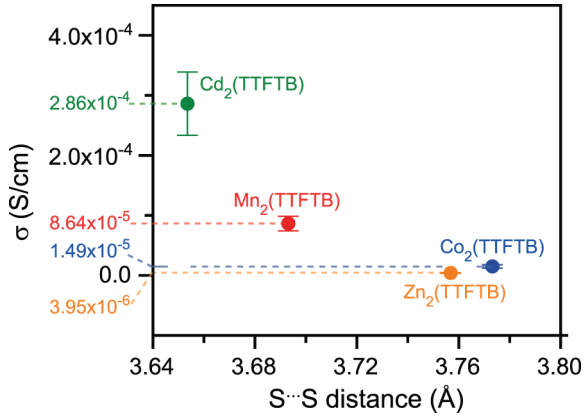


**Figure 4.** Correlation between S···S distance and electrical conductivity in $M_2$(TTFTB).

contact resistances are not responsible for the observed differences among the four analogues. The consistently smaller size of the $Zn_2$(TTFTB) crystals prevented us from performing a similar experiment on this material. On the other hand, measurement of the single-crystal conductivity of $Zn_2$(TTFTB) in a direction perpendicular to the *c* axis, performed by attaching two gold leads parallel to the *ab* plane (see Figure S9), revealed a value of 2.03 × $10^{-7}$ S/cm. Thus, the conductivity of $M_2$(TTFTB) is anisotropic and is largest along the direction of the TTF column. Overall, the conductivity values of all $M_2$(TTFTB) are among the highest for any microporous coordination polymer.

In conclusion, we showed that using increasingly larger cations causes an elongation of the one-dimensional SBUs and a concomitant contraction of the inter-TTF distance in


DOI: 10.1021/ja512437u
J. Am. Chem. Soc. 2015, 137, 1774−1777

$M_2$(TTFTB), a series of MOFs with $\pi$-stacked TTF columns. By decreasing the S···S distance between neighboring TTF cores, we were able to increase the overlap between the sulfur $3p_z$ orbitals, which are critically involved in the charge transport pathway, as revealed by DFT calculations. This led to the isolation of a series of new, permanently porous MOFs with high intrinsic conductivity and an improvement of nearly two orders of magnitude for $Cd_2$(TTFTB) over the original analogous zinc compound. These results provide a systematic blueprint for designing new electrically conductive MOFs based on the through-space charge transport formalism.

## ■ ASSOCIATED CONTENT

### Supporting Information

Detailed experimental procedures and computational details, X-ray crystal data (PXRD and single crystal), $N_2$ adsorption isotherms, conductivity measurements, and TGAs. This material is available free of charge via the Internet at http://pubs.acs.org.

## ■ AUTHOR INFORMATION


### Corresponding Author

mdinca@mit.edu


### Notes

The authors declare no competing financial interest.

## ■ ACKNOWLEDGMENTS

All experimental work was supported by the U.S. Department of Energy, Office of Science, Office of Basic Energy Sciences (U.S. DOE-BES, Award No. DE-SC0006937). S.S.P. is partially supported by a NSF GRFP (Award No. 1122374). Computational work at MIT was supported as part of the Center for Excitonics, an Energy Frontier Research Center funded by the U.S. DOE-BES (Award No. DE-SC0001088). T.V.V. thanks the David and Lucille Packard Foundation for a Fellowship. Work in the UK benefited from access to ARCHER through membership of the UK's HPC Materials Chemistry Consortium, which is funded by EPSRC (Grant No. EP/L00202). We thank M. Campbell and C. Brozek for helpful discussions, and T. Narayan for initial crystallization experiments. M.D. also thanks the Sloan Foundation, the Research Corporation for Science Advancement (Cottrell Scholar), and 3M for nontenured faculty support.

## ■ REFERENCES


(1) (a) Furukawa, H.; Cordova, K. E.; O'Keeffe, M.; Yaghi, O. M. *Science* **2013**, *341*, 1230444. (b) He, Y.; Zhou, W.; Qian, G.; Chen, B. *Chem. Soc. Rev.* **2014**, *43*, 5657. (c) Sumida, K.; Rogow, D. L.; Mason, J. A.; Mcdonald, T. M.; Bloch, E. D.; Herm, Z. R.; Bae, T.-H.; Long, J. R. *Chem. Rev.* **2012**, *112*, 724. (d) Suh, M. P.; Park, H. J.; Prasad, T. K.; Lim, D.-W. *Chem. Rev.* **2012**, *112*, 782. (e) Wu, H.; Gong, Q.; Olson, D. H.; Li, J. *Chem. Rev.* **2012**, *112*, 836. (f) Li, J.-R.; Sculley, J.; Zhou, H.-C. *Chem. Rev.* **2012**, *112*, 869. (g) Murray, L. J.; Dincă, M.; Long, J. R. *Chem. Soc. Rev.* **2009**, *38*, 1294.

(2) (a) Jin, S.; Son, H.-J.; Farha, O. K.; Wiederrecht, G. P.; Hupp, J. T. *J. Am. Chem. Soc.* **2013**, *135*, 955. (b) Coronado, E.; Espallargas, G. M. *Chem. Soc. Rev.* **2013**, *42*, 1525. (c) Ameloot, R.; Aubrey, M.; Wiers, B. M.; Gómora-Figueroa, A. P.; Patel, S. N.; Balsara, N. P.; Long, J. R. *Chem.—Eur. J.* **2013**, *19*, 5533. (d) Bag, S.; Gaudette, A. F.; Bussell, M. E.; Kanatzidis, M. G. *Nat. Chem.* **2009**, *1*, 217. (e) Zheng, N.; Bu, X.; Feng, P. *Nature* **2003**, *426*, 428. (f) Dechambenoit, P.; Long, J. R. *Chem. Soc. Rev.* **2011**, *40*, 3249.

(3) (a) Stavila, V.; Talin, A. A.; Allendorf, M. D. *Chem. Soc. Rev.* **2014**, *43*, 5994. (b) Allendorf, M. D.; Schwartzberg, A.; Stavila, V.; Talin, A. A. *Chem.—Eur. J.* **2011**, *17*, 11372.

(4) (a) Avendano, C.; Zhang, Z.; Ota, A.; Zhao, H.; Dunbar, K. R. *Angew. Chem., Int. Ed.* **2011**, *50*, 6543. (b) Cui, J.; Xu, Z. *Chem. Commun.* **2014**, *50*, 3986. (c) Hmadeh, M.; Lu, Z.; Liu, Z.; Gándara, F.; Furukawa, H.; Wan, S.; Augustyn, V.; Chang, R.; Liao, L.; Zhou, F.; Perre, E.; Ozolins, V.; Suenaga, K.; Duan, X.; Dunn, B.; Yamamto, Y.; Terasaki, O.; Yaghi, O. M. *Chem. Mater.* **2012**, *24*, 3511. (d) Takaishi, S.; Hosoda, M.; Kajiwara, T.; Miyasaka, H.; Yamashita, M.; Nakanishi, Y.; Kitagawa, Y.; Yamaguchi, K.; Kobayashi, A.; Kitagawa, H. *Inorg. Chem.* **2009**, *48*, 9048. (e) Kambe, T.; Sakamoto, R.; Hoshiko, K.; Takada, K.; Miyachi, M.; Ryu, J.-H.; Sasaki, S.; Kim, J.; Nakazato, K.; Takata, M.; Nishihara, H. *J. Am. Chem. Soc.* **2013**, *135*, 2462. (f) Sun, L.; Miyakai, T.; Seki, S.; Dincă, M. *J. Am. Chem. Soc.* **2013**, *135*, 8185.

(5) (a) Wiers, B. M.; Foo, M.-L.; Balsara, N. P.; Long, J. R. *J. Am. Chem. Soc.* **2011**, *133*, 14522. (b) Talin, A. A.; Centrone, A.; Ford, A. C.; Foster, M. E.; Stavila, V.; Haney, P.; Kinney, R. A.; Szalai, V.; Gabaly, F. E.; Yoon, H. P.; Léonard, F.; Allendorf, M. D. *Science* **2014**, *343*, 66.

(6) (a) Dong, H.; Fu, X.; Liu, J.; Wang, Z.; Hu, W. *Adv. Mater.* **2013**, *25*, 6158. (b) Grozema, F. C.; Siebbeles, L. D. A. In *Charge and Exciton Transport through Molecular Wires*; Siebbeles, L. D. A., Grozema, F. C., Eds.; Wiley-VCH; Weinheim, Germany, 2011; Chapter 9.

(7) Hoffmann, R. *Acc. Chem. Res.* **1971**, *4*, 1.

(8) Batra, A.; Kladnik, G.; Vázquez, H.; Meisner, J. S.; Floreano, L.; Nuckolls, C.; Cvetko, D.; Morgante, A.; Venkataraman, L. *Nat. Commun.* **2012**, *3*, 1086.

(9) Sirringhaus, H.; Brown, P. J.; Friend, R. H.; Nielsen, M. M.; Bechgaard, K.; Langeveld-Voss, B. M. W.; Spiering, A. J. H.; Janssen, R. A. J.; Meljer, E. W.; Herwig, P.; de Leeuw, D. M. *Nature* **1999**, *401*, 685.

(10) Yoshizawa, K. *Acc. Chem. Res.* **2012**, *45*, 1612.

(11) (a) Marcus, R. A. *Angew. Chem., Int. Ed. Engl.* **1993**, *32*, 1111. (b) Winkler, J. R.; Gray, H. B. *J. Am. Chem. Soc.* **2014**, *136*, 2930.

(12) (a) Narayan, T. C.; Miyakai, T.; Seki, S.; Dincă, M. *J. Am. Chem. Soc.* **2012**, *134*, 12932. (b) Saeki, A.; Koizumi, Y.; Aida, T.; Seki, S. *Acc. Chem. Res.* **2012**, *45*, 1193.

(13) Gándara, F.; Uribe-Romo, F. J.; Britt, D. K.; Furukawa, H.; Lei, L.; Cheng, R.; Duan, X.; O'Keeffe, M.; Yaghi, O. M. *Chem.—Eur. J.* **2012**, *18*, 10595.

(14) Kobayashi, Y.; Jacobs, B.; Allendorf, M. D.; Long, J. R. *Chem. Mater.* **2010**, *22*, 4120.

(15) (a) Sproules, S.; Wieghardt, K. *Coord. Chem. Rev.* **2011**, *255*, 837. (b) Eisenberg, R.; Gray, H. B. *Inorg. Chem.* **2011**, *50*, 9741. (c) Cui, J.; Xu, Z. *Chem. Commun.* **2014**, *50*, 3986. (d) Hmadeh, M.; Lu, Z.; Liu, Z.; Gándara, F.; Furukawa, H.; Wan, S.; Augustyn, V.; Chang, R.; Liao, L.; Zhou, F.; Perre, E.; Ozolins, V.; Suenaga, K.; Duan, X.; Dunn, B.; Yamamto, Y.; Terasaki, O.; Yaghi, O. M. *Chem. Mater.* **2012**, *24*, 3511.

(16) Sheberla, D.; Sun, L.; Blood-Forythe, M. A.; Er, S.; Wade, C. R.; Brozek, C. K.; Aspuru-Guzik, A.; Dincă, M. *J. Am. Chem. Soc.* **2014**, *136*, 8859.

(17) Hoffmann, R. *Angew. Chem., Int. Ed. Engl.* **1987**, *26*, 846.

(18) (a) Pham, H. Q.; Mai, T.; Pham-Tran, N.-N. *J. Phys. Chem. C* **2014**, *118*, 4567. (b) Musho, T.; Li, J.; Wu, N. *Phys. Chem. Chem. Phys.* **2014**, *16*, 23646. (c) Yang, L.-M.; Fang, G.-Y.; Ma, J.; Ganz, E.; Han, S. S. *Cryst. Growth Des.* **2014**, *14*, 2532.

(19) Kreno, L. E.; Leong, K.; Farha, O. K.; Allendorf, M.; Van Duyne, R. P.; Hupp, J. T. *Chem. Rev.* **2012**, *112*, 1105.

(20) Butler, K. T.; Hendon, C. H.; Walsh, A. *J. Am. Chem. Soc.* **2014**, *136*, 2703.

(21) Shannon, R. D. *Acta Crystallogr.* **1976**, *A32*, 751.

(22) Blessing, R. H.; Coppens, P. *Solid State Commun.* **1974**, *15*, 215.

(23) Aumüller, A.; Erk, P.; Hünig, S.; von Schütz, J. U.; Werner, H.-P.; Wolf, H. C.; Klebe, G. *Chem. Ber.* **1991**, *124*, 1445.

(24) Williams, R.; Lowe, M. C.; Samson, S.; Khanna, S. K.; Somoano, R. B. *J. Chem. Phys.* **1980**, *72*, 3781.

(25) (a) Pop, F.; Auban-Senzier, P.; Frąckowiak, A.; Ptaszyński, K.; Olejniczak, I.; Wallis, J. D.; Canadell, E.; Avarvari, N. *J. Am. Chem. Soc.* **2013**, *135*, 17176. (b) Augusto, D.; Marzotto, A. *J. Mater. Chem.* **1996**, *6*, 941.

(26) Givaja, G.; Amo-Ocha, P.; Gómez-García, C. J.; Zamora, F. *Chem. Soc. Rev.* **2012**, *41*, 115.




DOI: 10.1021/ja512437u
*J. Am. Chem. Soc.* 2015, 137, 1774−1777